

# Improving the measurement of thread parameters by use of corundum elements

E V Leun

Lavochkin Association, 24 str. Leningradskaya, Khimki, 141402, Russia

**Abstract.** Considered an advanced method of the three wires to measure the average diameter  $d_{av}$  and pitch  $P$  of the thread using three elements corundum (synthetic sapphire, sapphire, ruby): two fibers and tip with the ability to visualize and measure the size of the contact zone with the product to calculate the contact elastic deformation. It is proposed to use two fibers incoherent and one coherent interferometers to measure the position of corundum fibers and the tip. A method for calculating the diameter  $d_{av}$  and pitch  $P$  of the thread based on the results of interferometer measurements by using the compensation of contact elastic deformations is presented.

## 1. Introduction

Threaded connections are widely used in products of rocket and space technology, aviation, shipbuilding, oil and gas production and other industries. Measurement of thread parameters is not an easy task and a large number of works abroad [1–5] and in Russia [6–14] are devoted to its solution. The required accuracy of thread measurement systems (TMS) can reach units of micrometers, sometimes causing submicron accuracy of the measuring instruments used.

The measuring tip is an important element and often determines the progress of the TMS itself [6, 7]. However, the main disadvantage of the existing tips is due to their so-called "blindness" due to the inability to visualize and measure the contact zone with the threaded surface, limiting the functionality and accuracy of measurements due to uncompensated contact elastic deformations (further -deformation).

## 2. Formulation of the problem

The task of this work is the improvement of methods and means of measurement of threads by the use of high strength and optically transparent elements corundum (synthetic sapphire, sapphire, ruby) with the ability to visualize the contact zone.

## 3. Theory

This chapter consist of descriptions developed TMS, its principle of operation, features measure the average diameter of  $d_{av}$  and pitch  $P$  with deformation compensation.

### 3.1. Device and principle of operation of the TMS with corundum tip and two fibers

It is known that the average diameter of the thread  $d_{av}$  is the diameter coaxial with the thread of the cylinder, which forming line crosses the profile of the thread at the points where the groove width is half the thread pitch  $P$ , which is equal to the distance between the adjacent sides of the same profile in the direction parallel to the thread axis. As you can see, to determine  $d_{av}$ , you need to measure  $P$ .



To measure the average diameter  $d_{av}$  and pitch  $P$  thread was developed TMS is shown on figure 1a,b with the compensation of deformations [15], consisting of a corundum measuring tip 1 (further – the tip) and two fibers 2 (installed in accessory) by highly coherent 3 and the two low-coherence fiber interferometers 4, each of which includes a fiber head 5 and GRIN lens 6 installed in the optical input. GRIN lens 6 is a radial gradient lens and has a quadratic change in the refractive index  $n_r = n_o(1 - \frac{Ar^2}{2})$ , where  $r$  is the distance from the optical axis of the lens,  $n_o$  – the axial refractive index, and  $A$  - a constant.

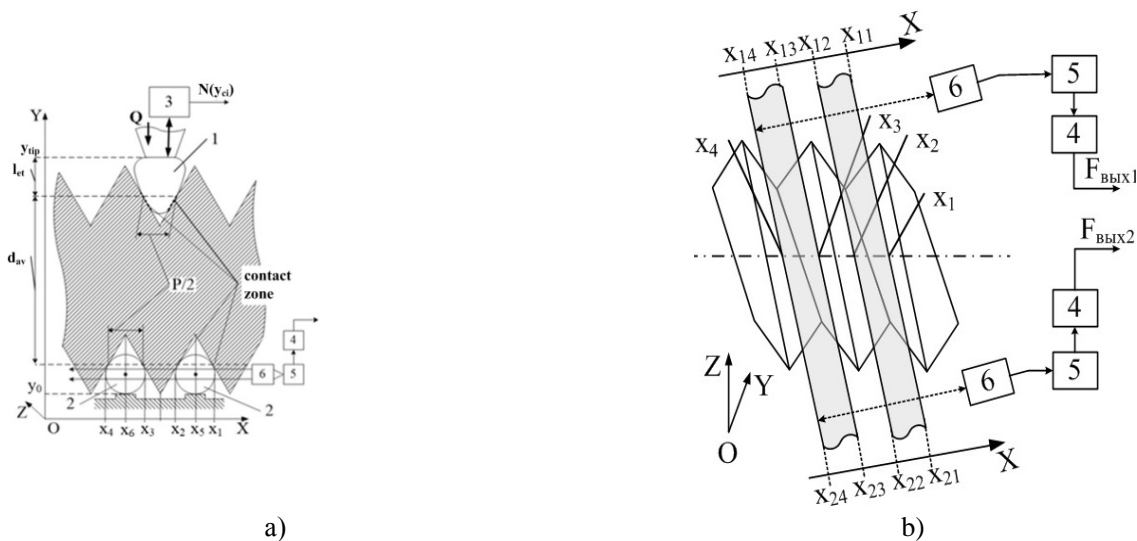


**Figure 1.** Contacting the corundum tip and the two fibers during measurement: in the plane of XOY (a) and ZOY (b).

Tip 1 (figure 2a,b) has a calibrated surface in the XOY plane with the measured dependence  $L_H = F(l_{et})$  of the thickness  $L_{tip}$  for the distance from its end  $l_{et}$  according to figure 2c. Therefore, the  $l_{et}$  value for a given  $L_{tip}$  value is determined by the inverse function

$$l_{et} = F^{-1}(L_{tip}). \tag{1}$$

The tip section 1 is close in shape to an isosceles triangle with spherical sides of radius  $R_{tip} \geq P$ , the value of which is sought to increase for raising the size of the contact zone  $l_{cz}$  in according to formula [15]:

$$l_{cz} = 2\sqrt{2 \cdot R_{tip} \cdot l_d - l_d^2}. \tag{2}$$

On top of the tip 1, immersed in the threaded cavity, additional small flat surfaces can be formed (figure 2b) to form a directed flow illuminating the sides of the tip 1 and register the contact zone in reflected light with a higher signal level. Tip 1 can have two lighting and registration channels (figure 2a) located along the tips of the tip, as well as two lighting channels illuminating emitters and one central recorder (figure 2b).

In the process of measuring the average diameter  $d_{av}$  and thread pitch  $P$  tip 1 and corundum fibers 2 are introduced from opposite sides into the threaded cavities of the product. The position of the tip 1 is determined by the displacement from the reference point by using a highly coherent interferometer 3 and the upper and lower edges of corundum fibers 2 by two fiber incoherent interferometers 4.

The recorder(s) 7 are optically coupled to the tip 1 by connected in series GRIN lens 11 and optical system 10. And the emitter(s) 8 are optically coupled to the tip 1 by the optical fibers 9. The recorder(s) 7 and the emitter(s) 8 are electrically coupled to the measuring scheme 12. In one of the variants (figure 2b) two emitters 8 with one common recorder 7 can be used. The use of these optical elements is determined by the

need to register and measure the size of the contact zone in direct illumination (figure 2a) or reflected (figure 2b) light.

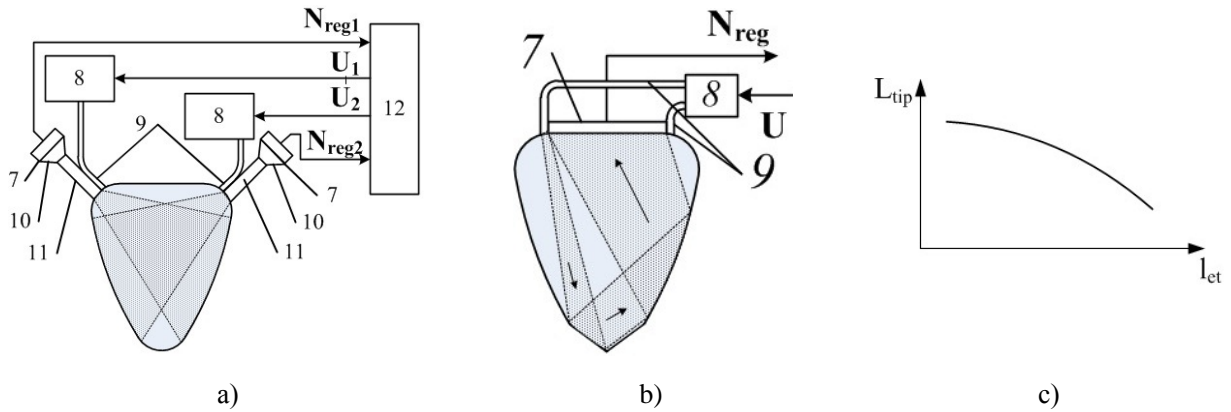


**Figure 2.** Electronic measuring scheme of the proposed method of measurement based on the corundum tip with the ability to visualize and record the contact zone: with direct illumination (a), in reflected light (b) and dependence  $L_{tip}=F(l_{et})$  of the thickness  $L_{tip}$  for the distance from its end  $l_{et}$  (c).

Each fiber head 5 by means of the built-in vibrating light guide emits a laser beam following through the GRIN lens 6 and deviating in the XOY plane in the angular range  $\pm\alpha$ . After GRIN lens 6, the angular deviations of the laser beam are transformed into linear displacements orthogonal to its axis, following through two transparent fibers 2. Each of the boundaries of the fibers 2 generates reflected light beams, which follow in the opposite direction through GRIN lens 6 and the fiber head 5 and interfering in incoherent interferometer 6, generates signals, which are determined by two groups of coordinates  $x_{11}, x_{12}, x_{13}, x_{14}$  and  $x_{21}, x_{22}, x_{23}, x_{24}$  for the top and bottom parts, respectively. The coordinates of the fiber's 2 boundaries in the XOY plane are calculated by the next formulas:  $x_1 = \frac{x_{11} + x_{21}}{2}$ ,  $x_2 = \frac{x_{12} + x_{22}}{2}$ ,  $x_3 = \frac{x_{13} + x_{23}}{2}$ ,

$x_4 = \frac{x_{14} + x_{24}}{2}$ , which allows to determine the thread pitch P based on the measured coordinates:

first group

$$P = x_3 - x_1 = \frac{x_{13} + x_{23}}{2} - \frac{x_{11} + x_{21}}{2} = \frac{1}{2}(x_{13} + x_{23} - x_{11} - x_{21}), \quad (3)$$

second group

$$P = x_4 - x_2 = \frac{x_{14} + x_{24}}{2} - \frac{x_{12} + x_{22}}{2} = \frac{1}{2}(x_{14} + x_{24} - x_{12} - x_{22}) \quad (4)$$

or averaging over two groups of measurements

$$P = \frac{(x_3 - x_1) + (x_4 - x_2)}{2} = \frac{x_{13} + x_{23} - x_{11} - x_{21} + x_{14} + x_{24} - x_{12} - x_{22}}{4}. \quad (5)$$

The obtained data, taking into account the known radius  $R_f$  of fibers 2, are used for further calculations.

### 3.2. Method of determining deformations and caused by them the measurement error of the average diameter of the thread

During the measurement process, a tip with spherical sides and two fibers with cylindrical surfaces contact with the helical surface. At the point of contact, the helical surface itself is spherical. However, due to the

fact that the forming surface of the threaded projections straightforward, and the thread pitch  $P$  is less than the average diameter of the thread  $d_{av}$ :  $P < d_{av}$ , but also because of the smallness of the size of the contact zone  $l_{cz}$  fibers with a helical surface, we assume that in all cases there is a contact of type "sphere-plane" and

the size of the contact zone is determined by the expression [15]:  $l_d = R_{tip} - \sqrt{R_{tip}^2 - \frac{l_{zc}^2}{4}}$ .

When contacting a spherical tip with an inclined plane (Figure 3) deformation  $l_d$  cause error  $\Delta l_{dt}$  – sections  $[O; O_1]$  or  $[A; B]$ , depending on the angle  $\gamma$  thread:

$$\Delta l_{dt} = \frac{l_d}{\sin \gamma} = k_\gamma \cdot l_d = k_\gamma \left( R_{tip} - \sqrt{R_{tip}^2 - \frac{l_{zc}^2}{4}} \right) \tag{6}$$

where  $k_\gamma = \text{cosec} \gamma$  - factor angle of the thread.

For symmetrical threads, the value  $\Delta l_{dt}$  the same for each side of the threaded cavity, but for asymmetric thread is not running. Values of measurement error  $\Delta l_{dt}$  calculated by the formula (2) shown in Table 1 for different angles of inclination for symmetrical and asymmetrical threads round, trapezoidal, tubular, metrical and persistent and persistent reinforced thread, respectively.

The measurement method of contact deformations is based on the following steps: measuring the dimensions of the contact areas of the tip → the first calculation of tip’s contact deformation → the second calculation of contact deformations for the two corundum fibers → the calculation of the total measurement error  $\Delta l_{d\Sigma}$  from the contact deformations of the tip  $\Delta l_{dt}$  and two corundum fibers  $\Delta l_{df}$  by the formula:

$$\Delta l_{d\Sigma} = \Delta l_{dt} + \Delta l_{df} \tag{7}$$

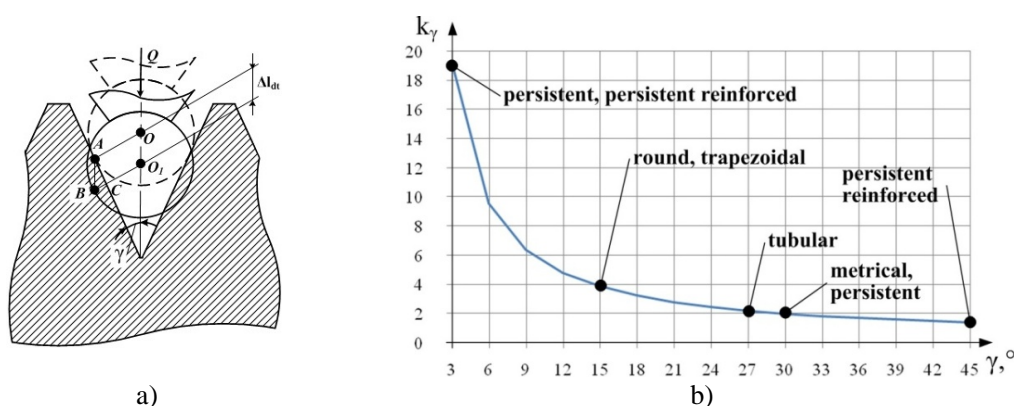


**Figure 3.** Formation of measurement error from deformations (a), the dependence of the coefficient  $k_\gamma$  on the thread’s angle of inclination  $\gamma$  (b).

**Table 1.** The value of measurement error  $\Delta l_{dt}$  for different angles of inclination.

N <sub>o</sub>	The symmetry of the thread	Thread type	Angle $\gamma, ^\circ$	Error $\Delta l$
1		round	15	$3,86l_d$
2	Symmetric	trapezoidal	15	$3,86l_d$
3	threads $\gamma_{II} = \gamma_3$	tubular	$27^\circ 30'$	$2,16l_d$
4		metrical	30	$2l_d$
5	Asymmetrical	persistent	30/3	$2l_d/19, 11d$
7	threads $\gamma_{II} \neq \gamma_3$	persistent reinforced	45/3	$1,4l_d/19, 11d$

For this measurement method of contact deformations , the following assumptions are made:

- contact deformations are linear for small measuring forces <10 N;
- the contact zone has a round shape, corresponding to the contact of the sphere with the plane;
- the strength parameters of the product and accessory, with installed cylindrical corundum fibers, are close in values.

In equilibrium, the measuring forces acting on the surface area of the tip and the two fibers are:  $\frac{F}{S_{\Sigma tip}} = \frac{F}{S_{\Sigma f}}$ ,

where  $S_{\Sigma tip} = S_{\Sigma f}$  and taking into account the fact that the area of the two contact zones of the tip  $S_{tip}$  according to figure 2 is equal to the area of eight contact areas  $2S_{tip}=8S_f$ ,  $\rightarrow S_{tip}=4S_f$ , four on each fiber: two contact areas for the product and two for accessory – for top and bottom part of the fibers. The value  $S_{tip}$  can be calculated using the formula for the area of the sector  $S_{tip}=2\pi R_{tip}l_{dt}$ , where  $R_{tip}$  and  $l_{dt}$  is the tip's radius and deformation from contact with the product.

Estimate of parameter  $S_f$  can be found similar  $S_f=2\pi R_f l_{df}$  where  $R_f$  and  $l_{df}$  is the radius of corundum fibers and its deformation from their contact with the product and accessory. Equating  $2S_{tip}$  and  $8S_f$  get  $4\pi R_{tip}l_{dt} = 16\pi R_f l_{df}$ , where have

$$l_{df} = \frac{R_{tip} \cdot l_{dt}}{4R_f} \quad (8)$$

and after substituting this expression in formula (2) we obtain an expression for error  $\Delta l_f$  from deformations of corundum fibers taking into account the angle  $\gamma$  of the thread:

$$\Delta l_{df} = \frac{l_{df}}{\sin \gamma} = k_\gamma \cdot l_{df} = \frac{k_\gamma \cdot R_{tip}}{4R_f} \left( R_{tip} - \sqrt{R_{tip}^2 - \frac{l_{zc}^2}{4}} \right) \quad (9)$$

Then, for the algebraic summation of errors by the formula (7) and according to the expressions (6) for  $\Delta l_{dt}$  and (9) for  $\Delta l_f$ , respectively, we obtain the total error from the contact deformations  $\Delta l_{d\Sigma}$ :

$$\Delta l_{d\Sigma} = \Delta l_{dt} + \Delta l_{df} = k_\gamma \left( R_{tip} - \sqrt{R_{tip}^2 - \frac{l_{zc}^2}{4}} \right) + \frac{k_\gamma \cdot R_{tip}}{4R_f} \left( R_{tip} - \sqrt{R_{tip}^2 - \frac{l_{zc}^2}{4}} \right) = k_\gamma \cdot \left( 1 + \frac{R_{tip}}{4R_f} \right) \cdot \left( R_{tip} - \sqrt{R_{tip}^2 - \frac{l_{zc}^2}{4}} \right) \quad (10)$$

Thus, the resulting expression represents two components of the measurement error caused by deformations  $\Delta l_{dt}$  and  $\Delta l_f$ , measured and subsequently compensated in this method.

### 3.3. Method for determining the average diameter of the thread $d_{av}$

The determination of the average diameter of the  $d_{av}$  is based on the calculation of two coordinates along the axis OY for the lower and upper forming (lines) according to figure 1a intersecting the thread profile at points dividing the thread pitch P in half. The position of the lower and upper generators is calculated using corundum fibers and a calibrated tip, respectively.

The calculation of the position of the lower generator is as follows. At equality of diameters of corundum fibers it is possible to write  $|AC| = |AB| = |A'C| = |A'B'| = \frac{|AD|}{\cos \gamma} = R_e \cdot \sec \gamma$  and then expression of width of a cavity  $l_{cav}$  takes the form:

$$l_{cav} = 2R_f \cdot \sec \gamma \quad (11)$$

The width of the ledge, as shown in figure 4,  $l_{led} = |B'C|$  is equal to the distance between the centers of the fibers  $|A'A|$  (or thread pitch P, defined earlier) except for the two halves of each cavity  $|A'B'|$  и  $|AC|$ , the sum of which is the width of the cavity:

$$l_{led} = |B'C| = P - |A'B'| - |AC| = P - 2R_f \cdot \sec \gamma. \quad (12)$$

The value of  $l_{lc}$  as the difference between the width of the ledge  $|B'C|$  and the width of the cavity  $l_{cav}$  determined by the formula

$$l_{lc} = l_{led} - l_{cav} = P - 2R_f \cdot \sec\gamma - 2R_f \cdot \sec\gamma = P - 4R_f \cdot \sec\gamma. \tag{13}$$

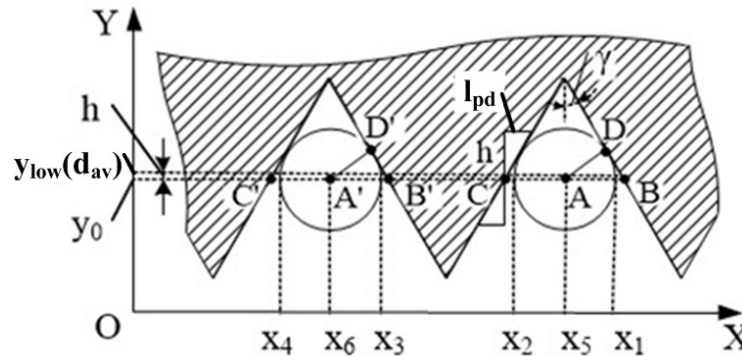


**Figure 4.** The location of corundum fibers in determining the coordinates of the axis OY corresponding to the lower generator in determining the average diameter  $d_{av}$ .

Implementation the condition  $l_{lc}=0$  means that the position of the line (BC') corresponds to the first coordinate on the axis OY of the lower boundary of the desired average diameter  $d_{av}$ . If we have the nonzero condition  $l_{lc} \neq 0$  there is a need to determine the displacement  $h$  to compensate one way or the other hand, the arising path difference between  $l_{led}$  and  $l_{cav}$ :  $l_{lc} = l_{pd}$  provided that the relationship between  $l_{pd}$  and  $h$  is given by  $l_{pd} = \pm h \cdot \text{tg}\gamma$

$$P - 4R_b \cdot \sec\gamma = \pm h \cdot \text{tg}\gamma. \tag{14}$$

When  $P - 4R_f \cdot \sec\gamma > 0$  the ledge is longer than the cavity ( $l_{led} > l_{cav}$ ) and when  $P - 4R_b \cdot \sec\gamma < 0$  – the opposite ( $l_{led} < l_{cav}$ ). Therefore, the displacement  $h$  with the positive direction of the axis OY, shown in figure 4, corresponds to the case with the formula  $P - 4R_b \cdot \sec\gamma = h \cdot \text{tg}\gamma$ , and so we can obtain  $h = \frac{P - 4R_f \cdot \sec\gamma}{\text{tg}\gamma}$ . And

then the formula for first coordinate is determined (the lower coordinate - according to figure 4)  $y_{low}(d_{av})$  on the axis OY, corresponding to the forming line of the average diameter:

$$y_{low}(d_{av}) = y_0 - h = y_0 - \frac{P - 4R_f \cdot \sec\gamma}{\text{tg}\gamma}, \tag{15}$$

where  $y_0$  is the position of the centers of corundum fibers.

The second coordinate (upper coordinate, shown in figure 1a)  $y_{top}(d_{av})$  on the axis OY, corresponds to the position of the forming line of the average diameter  $d_{av}$  for the tip thickness equal to half the thread pitch  $P$  according to (1)

$$l_{et} = F^{-1}\left(\frac{P}{2}\right). \tag{16}$$

The coordinate  $l_{et}$  is shifted from the tip's top apex with the  $y_{tip}$  coordinate, the position of which is measured by a highly coherent interferometer  $y_{ci}$  (figure 1a):

$$y_{top}(d_{av}) = y_{ci} + l_{et}. \tag{17}$$

Thus, the final formula for calculating the average diameter of the thread  $d_{av}$ , with formulas (5), (15) and (17) will take the form:

$$d_{av} = y_{top}(d_{av}) - y_{low}(d_{av}) + \Delta l_{d\Sigma} \tag{18}$$

### 3.4. Estimation of accuracy parameters of the developed TMS

Detailed metrological analysis, including analysis of temperature error, is beyond the scope of this publication and will be presented in next publications. However, a simplified estimation of the accuracy parameters of the developed TMS can be made to understand the planned measurement errors.

Determination of the thread pitch  $P$  is based on measurements by fiber incoherent interferometers, the accuracy of which can be at the level of  $0.5 \mu\text{m}$  [15, 16].

Then, taking into account the independent four measurements with an accuracy of  $0.5 \mu\text{m}$ , the partial differential expressions  $P$  for the arguments  $x_{11}, x_{13}, x_{21}, x_{23}$  of the formula (3) and their geometric addition obtain  $\Delta P = \sqrt{0.25^2 + 0.25^2 + 0.25^2 + 0.25^2} = 0.5 \mu\text{m}$ .

As follows from the expression (15) the greatest influence on the error of determining the lower coordinate of the  $\Delta y_{low}(d_{av})$  has  $\Delta P$ , the value of which, as shown above, can reach  $0.5 \mu\text{m}$ . In this case, the error  $\Delta \gamma$  can be neglected, taking it negligibly small.

The error in determining the upper coordinate of the  $\Delta y_{up}(d_{av})$  is determined by the deviation of the tip shape and for modern high-resolution measuring profilometers, this value can also be no higher than  $0.5 \mu\text{m}$ . The measurement accuracy of the laser interferometer is very small. Thus, modern acousto-optic displacement interferometers, reaching a resolution of  $\approx \lambda/1000$  [17,18] with the possibility of increasing to  $\approx \lambda/3000$  [19], allow to reduce the measurement error to  $0.01 \mu\text{m}$  and below. Thus, assuming that  $\Delta d_{av} = \sqrt{\Delta y_n^2(d_{av}) + \Delta y_g^2(d_{av})} = \sqrt{0.5^2 + 0.5^2} \approx 0.7 \mu\text{m}$ . As can be seen, the use of modern fiber low-coherence interferometers in the developed TMS allows to achieve submicron accuracy in measuring the pitch  $P$  and the average diameter  $d_{av}$  thread.

#### 4. Experimental result

Earlier in [14] the problems of visualization and experimental video recording of contact zones of a transparent flat body with an elastic product were considered. This to some extent can be considered an imitation of corundum contact with metals. And in figure 5 an image of a similar contact zone of a circular shape is presented, for which the radius and position of the center can be determined in determining the geometric parameters of the equation of the circle by means of various computer image processing

algorithms, for example, based on the method of least squares  $(x - x_0)^2 + (y - y_0)^2 = \left(\frac{l_{\text{яс}}}{2}\right)^2$ .

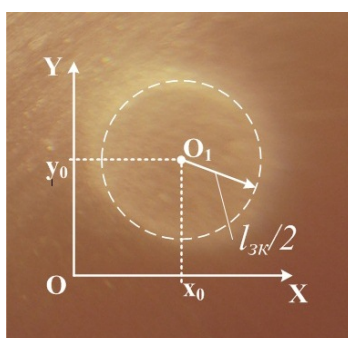


**Figure 5.** Photo of the contact zone of round shape and determination of its center

The main blocks of the developed TMS are well investigated. Sapphire rods of the desired shape can be grown by Stepanov method. Their minimum diameter can reach  $1.0 \dots 1.2 \text{ mm}$  [20, 21]. Fiber heads, having a diameter of  $\varnothing \approx 1.2 \text{ mm}$  and a length of  $9 \text{ mm}$ , are quite small and are already actively used as micro-projectors [22], microscanners and medical endoscopy [23–26].

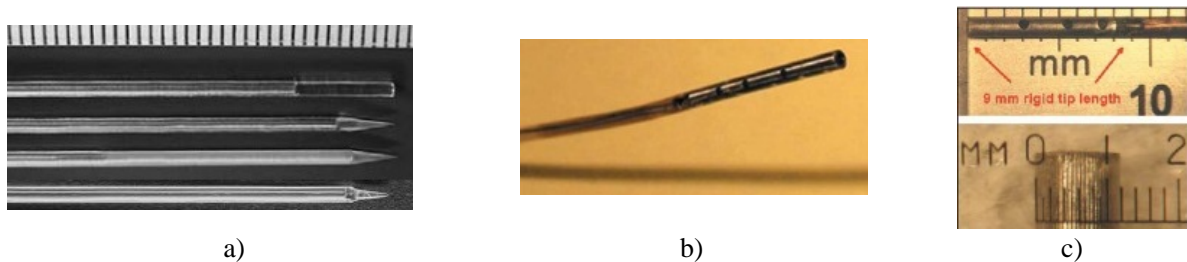


**Figure 6.** General view of the main elements TMS: sapphire fibers grown by the Stepanov (a) and the fiber head used in the fiber incoherent interferometer (b, c).

### 5. The discussion of the results

1. The use of high-strength and optically transparent corundum tip and two fibers, as well as one high-coherence and two low-coherence interferometers allows to improve the widely known method of measuring the threaded parameters of the "three wires" when measuring the average diameter  $d_{av}$  and the pitch  $P$  for thread by compensating contact deformations and improving the accuracy of measurements, approaching the submicron level.
2. Tip design with a cross section close to the triangle with spherical sides  $R_{tip}$  allows to increase the size of the contact zone. Measurement of contact deformation defined by this tip is recalculates to corundum fibers, allowing to estimate the total deformations and in total to compensate its from general measurements results.

### 6. Conclusion

The developed system continues the general trend of improvement of TMS initiated by recent works [1–13]. A distinctive feature of this development is the aspiration to visualize the contact zones by using of high-strength and optically transparent corundum tip and two fibers, allowing to apply of high-resolution optical measurement systems (interferometers). A further development of the TMS can be considered to increase the accuracy of measurements while simplifying its entire design.

### 7. References

- [1] Merkač T, Acko B 2010 Thread gauge calibration for industrial applications *J. Mechanical Engineering* **56** pp 637–643
- [2] Sheng C, Dongbiao Z, Yonghua L 2014 A new compensation method for measurement of thread pitch diameter by profile scanning *Measurement Science Review* vol **14** 6 pp 323–330
- [3] Galestien I 2007 Advanced 2d Scanning: the solution for the calibration of thread ring and thread plug gauges *Proc. 13th Intern. Metrology Congress (Lille)* pp 363–372
- [4] Tong Q, Jiao C, Huang H et al 2014 An automatic measuring method and system using laser triangulation scanning for the parameters of a screw thread *Measurement Science and Technology* **25** (3)
- [5] Tong Q, Ding Z, Chen J et al 2006 The research of screw thread parameter measurement based on position sensitive detector and laser *Journal of Physics* **48** pp 561–565
- [6] Leun V and Nikolaeva E 2015 Direct measurement of the mean thread diameter of cutting and monitoring tools in thread grinding *Russian engineering research* **2** (35) pp156–157
- [7] Leun V and Nikolaeva E 2015 Design of active monitoring systems for the mean thread diameter in thread grinding *Russian engineering research* **4**(35) pp 313–314
- [8] Kuvaldina A Pimneva N and Nikolaeva E 2017 *Measurements of threaded parts, gears and gears on coordinate measuring machines* (Omsk: Omsk State Technical University) pp 32–33
- [9] Zakharenko Y, Kononova N, Moskalev A 2016 Measurements of the Geometric Parameters of Thread Gauges *Measurement Techniques* vol **59** 2 pp 137–141

- [10] Moskalev A 2014 High-accurate measurements of thread gages using the Labconcept NANO horizontal instrument *Proc. 24 th Nat. scient. Symp. Intern. Particip. (Sozopol)* pp 480-485
- [11] Noskova Y, Khalturin O, Ablyaz T 2012 Control method of tapered thread for drill string elements on a coordinate measuring machine *Bulletin of Perm nat. res. Polytechnic University* vol **14** pp 85-91
- [12] Zubarev Y, Kosarevsky S, Tyrs V 2013 *Measuring thread features using coordinate measuring machines Izvestia VolgogradSTU* **7** (110) pp 22-25
- [13] Ostapchuk V, Kulikov V, Semenov S 2018 *Automated control of thread parameters* Website of the Niizmereniya URL: <http://www.micron.ru/information/articles/2> (date accessed: 15.09.2019).
- [14] Leun E, Shakhnov A, Nickel A 2019 Opportunities to increase the accuracy of contact measurements using corundum tips and video recording of the contact area *Omsk Scientific Bulletin* **2**(164) pp 68–75 DOI: 10.25206/1813-8225-2019-164-68-75
- [15] Akhsakhalyan A, Akhsakhalyan A, Volkov P et al 2015 Prospects of application of the tandem low-coherence interferometry method for measuring the shape of aspheric surfaces *Surface. X-ray, synchrotron and neutron studies* **8** pp 16-20
- [16] Volkov P, Goryunov A, Lukyanov A et al 2017 Measuring the surface profile of extended aspheric objects *Nanophysics and nanoelectronics: Proc. XXI intern. Symp. Vol 1* pp 379–380
- [17] Myshev V, Kapezin S, Ignatov S 1990 *Increase resolution interferometric linear encoder* (Penza: Penza State Technical University Press) pp 12-13
- [18] Grishin S 2011 Estimating phase errors in heterodyne laser interferometer measurement systems *Measurement Techniques* **548** pp 865–868
- [19] Leun E 2002 Features of design of acousto-optic laser system for measuring displacement with phase-digital conversion *Mechanical engineering Technology* vol **5** pp 33-40
- [20] Shikunova I, Volkov V, Kurlov V et al 2009 Sapphire needle capillaries for laser medicine *Proc. Russian Academy of Sciences. Series physical* vol **73** 10 pp 1424-1428
- [21] Shikunova I, Kurlov V, Stryukov D et al 2015 *New medical laser-fiber devices and instruments based on profiled sapphire crystals* Actual problems of condensed matter physics: sat. St. (Ekaterinburg: Ural's department of Russian Academy of Sciences Press) pp 31–46
- [22] Samarin A 2008 Laser micro-projector with spiral scan *Components and technologies* **10** pp 101–104
- [23] Huland D, Brown C, Howard S, Ouzounov D et al 2012 In vivo imaging of unstained tissues using long gradient index lens multiphoton endoscopic systems *Biomedical optics express* vol **3** 5 pp 1077–1085
- [24] Jung J, Schnitzer M 2003 Multiphoton endoscopy *Optics letters* vol **28** 11 pp 902-904
- [25] Huland D, Charan K, Ouzounov D et al 2013 Three-photon excited fluorescence imaging of unstained tissue using a GRIN lens endoscope *Biomedical optics express* **4** 5 pp 652-658
- [26] Schowengerdt B, Johnston R, Melville C and el 2012 3D Displays using scanning laser projection SID Symposium Digest of Technical Papers vol 43 pp 640–643